applied sciences

MDPI

Article

Evaporation of Water/Alumina Nanofluid Film by Mixed Convection Inside Heated Vertical Channel

A. Belhadj Mohamed [1,2], Walid Hdidi [3] and Iskander Tlili [4,5,*]

1 Deanship of the Preparatory Year, Umm Al Qura University, Makkah 21955, Saudi Arabia; amine.belhadj.m@gmail.com
2 Laboratoire d'Etudes des Systèmes Thermiques et Energétiques, Ecole Nationale D'Ingénieurs de Monastir, Monastir 5000, Tunisia
3 Department of mathematics, College of Arts and Sciences of Tabrjal, Jouf University, Sakaka 72341, Saudi Arabia; whadidi@ju.edu.sa
4 Department for Management of Science and Technology Development, Ton Duc Thang University, Ho Chi Minh City 758307, Vietnam
5 Faculty of Applied Sciences, Ton Duc Thang University, Ho Chi Minh City 758307, Vietnam
* Correspondence: iskander.tlili@tdtu.edu.vn

Received: 26 January 2020; Accepted: 18 March 2020; Published: 31 March 2020

Abstract: In industrial devices like heat recovery systems, heat pumps, as well as symmetric and complex engineering systems, a nano fluid mixture is used. Regarding the nature of the energy sources (thermal or thermal and electrical), many physical systems could represent possible applications in manufactural activities. The presence of nanoparticles inside a solvent is of great interest in order to optimize the efficacy of the nano-technology systems. The present work deals with heat and mass transfer through a vertical channel where an alumina/water film mixture flows on one of its plates. For simulation, we use a numerical method under mixed convection during water/alumina nano fluid evaporation. We heat the flown plate uniformly while the other is dry and exchange heat with a constant coefficient. The gas mixture enters channel with a constant profile. Results show that an augmentation of the volume rate of the nanoparticle disadvantages evaporation if the heating is absent. Otherwise, if the heating exists, an increasing volume rate of the nanoparticle advantages evaporation. We found also that the film velocity behavior when the volume rate of the nanoparticle varies, independent of the heating.

Keywords: liquid film; nano fluid; nanoparticle; evaporation; vertical channel

1. Introduction

Because of its small thickness, the evaporation of thin film provides high heat transfer rates. This phenomenon appears in micro heat pumps, MEMS systems (Microelectromechanical Systems), and in modern applications of nanotechnology devices (Wang et al. [1]; Plawsky et al. [2]). As an efficient cooling liquid, nano fluid enhances the transport of heat during thin film evaporation (Do and Jang [3]). Micro channel configuration study of nano fluid presence effects on the transfers was performed by Jun-Jie Zhao et al. [4]. It was shown that the nano fluid thermophysical property effect is mainly due to thermal conductivity enhancement. They conclude that increasing Cu-volume fraction engenders that condensation augments and consequently Cu-solutions becomes more stable.

Other works concerned the investigation of the thermophysical properties of the nano fluids. Choi [5] showed the amelioration of the conductivity by introducing nanoparticles. A protocol of measuring the thermal conductivity of a nano fluids was performed by Lee et al. [6]. By using a hot-wire apparatus, Xuan and Li [7] evaluated the thermal conductivity of mixture of liquid film and

nanoparticles. Also, to predict the thermal conductivity of mixture of liquid film and nanoparticles, Xuan and Roetzel [8] suggested two different protocols. Ali et al. [9] investigated the transfer of heat and mass through a falling solution. They found controversial results, which suggest having a big base of data.

Several other works studied the hydrodynamic and thermal behavior of nano fluid numerically and experimentally in confined flows. Pak and Cho [10] observed the transfer of heat by forced convection when a tube is heated for several Reynolds numbers. They prove that the coefficient of convective heat transfer enhances with the volume rate of nanoparticles. To evaluate the Nusselt number when the regime is turbulent, they provide an approximate correlation. Experimental investigation of the heat transfer and the characteristics of flow in a tube, heated externally with a constant flux, is performed by Li and Xuan [11]. The collected data of the mixtures: (water and Cu, TiO_2 particles) and (water and Al_2O_3 particles), provided an empirical correlation for the Nusselt number. Theses approximations were given when the flows are laminar and turbulent. Under laminar flow regime, the intensity of the heat transfer through a water-Al_2O_3 mixture is studied by Wen and Ding [12]. For copper tube, they found that an augmentation of Reynolds number and the nano fluid volume concentration ameliorate the heat transfer coefficient by convection. Yang et al. [13] experimentally evaluated the transfer of heat by the convection of nano fluids formed of transmission fluids and graphitic-based nanoparticles. It is shown that the presence of nanoparticles engenders a real augmentation of the heat transfer through the physical systems. Fohanno. et al. [14] presented a critical investigation of the different numerical methods to compute the thermophysical properties of several nano fluids [15–19].

By using a pendant droplet method, Chen et al. [20] evaluated the tension of surface relative to a three types of nano fluid (laponite-water, silver-water and Fe_2O_3-water). Orejon et al. [21] studied nano fluid droplets evaporating under DC conditions. They revealed several evolutions relative to contact angle, deposit patterns and contact radius. It is shown that if we apply the DC potential, the TiO_2 nano fluids receding contact is smooth and continuous. Also, the deposit patterning is uniform. Furthermore, the nanoparticles interactions are different compared to the DC potential case. Ni et al. [22] tested the evaporation of nano fluid based on solar energy. They show that the performance of this system is around 69% relative to the nano fluid evaporation and the transient phase change depends on the nanoparticles surface chemistry. In addition, they use the Fourier law to model the thermal attitude of the nano fluid at microscale. In the same field, Amjad et al. [23] used gold nanoparticles to generate steam under solar heating. They demonstrate that a cooled bulk fluid causes an important surface of evaporation and they evaluate the photothermal performance by integrating a new method. They demonstrate, experimentally, that a 0.04% of gold in volume increases the evaporation rate by 95%. Zhou et al. [24] analyzed the absorption and desorption of molecules of fluid in a porous media formed by nanoparticles. Their numerical results are consistent with experimental data and prove that we can modify the properties of the energy storage by exothermic and endothermic adsorption and desorption. Moshizi [25] studied the influence of a constant magnetic field in the heat and mass transfer through a micro channel in presence of cu-water nano fluid. The Brinkman model allowed him to investigate the problem and to transform the nonlinear equations to the simple linear system. Moshizi et al. [26] gave a theoretical study of the convective transfer of heat taking into account the pressure drop. They consider the effect of the nanoparticle volume rate by using the Buongiorno model. S. A. Moshizi [27] studied the influence of the (MHD) field on the developed forced convection of heat with nano fluid in pipes. S. A. Moshizi and A. Malvandi [28] looked mathematically for the effect of an external magnetic field on the nanoparticles motion. Their study was during a mixed gas convection inside micro-channels. They consider the effect of the nanoparticle volume rate by using the Buongiorno model. The same authors [29] related the effect of the nano particles migration on the heat exchangers efficiency. With changing the migration modes of the Al_2O_3 inside water and under the mixed convection of gas in vertical micro channels, they demonstrate the influence of the thermophysical variations on the heat transfer. S. A. Moshizi et al. [30] present a study of magnetic field direction on transfers. They vary this direction in the case of the (MHD) nano fluids in isothermal micro tubes. This (MHD) phenomena was

investigated when the nano fluid is electrically conductive in micro annuli [31]. M. Sohail et al. [32] analysis the entropy relative a Maxwell nano fluid by modifying the heat and mass transfer models. Also, the generalize the law of Fick. I. M. Eldesoky et al. [33] showed that position and time affect the magnetic field influence on the temperature of nano fluid. S. I. Abdelsalam et al. [34] studied the unsteady peristaltic motion of a non-Newtonian nano fluid. They show the influence of a magnetic field and the currents of Hall. In addition, they take into the account the chemical reaction.

Regarding the previous studies, no study has given interest to the behavior of nano fluids in a semi-confined area like vertical channel. It will be the objective of this present work when no external heat is provided (heated flown plate case).

2. Analysis

This work provides a simulation study of heat and mass transfer when evaporation by mixed convection in a vertical channel (Figure 1) formed by two parallel plates. We heat the flown one with a constant flux. An alumina-water nano fluid is falling down in the presence of descending laminar mixed convection flow. The second plate is dry and exchanges heat with environment. The thermophysical properties of the nano fluid are obtained from [14] and those of the humid air from [15].

I. The nano film enters the channel with a temperature T_{nf0}, a thickness δ_0 and a velocity u_{nf0}. The air enters with a temperature T_0, mass fraction vapor c_0 and a velocity u_0. Assumptions are used to build up the mathematical system of the problem.
II. The flows through the vertical channel are laminar and stationary (gas and film). The study of the transfers is in two-dimensional case.
III. The nano film is considered as a boundary layer.
IV. Humid air is considered as an ideal mixture and perfect gas.
V. We don't take into the account the surface tension.
VI. The gas–nano fluid interface is in the thermodynamic equilibrium.
VII. We neglect the Soret and Duffour effects.
VIII. In the energy equation, we don't consider the pressure work terms, Radiation heat transfer and the viscous dissipation.

Firstly, we will present the general equations of conservation. Then, the boundary conditions equations will be presented in detail.

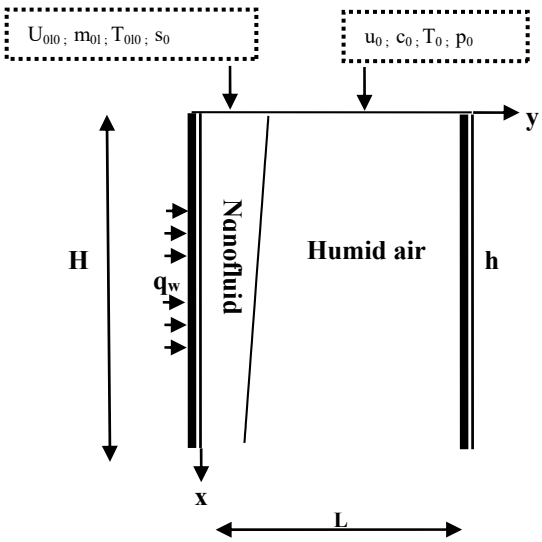

Figure 1. Physical System.

2.1. General Equations

The heat and mass transfer for the laminar mixed convection induced by the combined thermal and mass buoyancy forces, introducing the following transformations:

In gas phase:

$$Y = (y - \delta)/(d - \delta);\ X = x/H \tag{1}$$

In liquid phase:

$$Y_{nf} = (y - \delta)/\delta;\ X = x/H \tag{2}$$

Adopting these transformations, the equations governing the flow and the heat and mass transfers in the liquid and gas phases are:

2.1.1. For Liquid Phase

Continuity equation

$$\frac{\partial \rho_{nf} u_{nf}}{\partial X} - \frac{Y_{nf}}{\delta}\frac{\partial \delta}{\partial X}\frac{\partial \rho_{nf} u_{nf}}{\partial Y_{nf}} + \frac{H}{\delta}\frac{\partial \rho_{nf} v_{nf}}{\partial Y_{nf}} = 0. \tag{3}$$

Momentum equation

$$u_{nf}\frac{\partial u_{nf}}{\partial X} + \left(u_{nf}\frac{Y_{nf}}{\delta}\frac{\partial \delta}{\partial X} + v_{nf}\frac{H}{\delta}\right)\frac{\partial u_{nf}}{\partial Y_{nf}} = \frac{H}{\rho_{nf}\delta^2}\frac{\partial}{\partial Y_{nf}}\left(\mu_{nf}\frac{\partial u_{nf}}{\partial Y_{nf}}\right) + gH \tag{4}$$

Energy equation

$$u_{nf}\frac{\partial T_{nf}}{\partial X}\left(u_{nf}\frac{Y_{nf}}{\delta}\frac{\partial \delta}{\partial X} + v_{nf}\frac{H}{\delta}\right)\frac{\partial T_{nf}}{\partial Y_{nf}} = \frac{H}{\rho_{nf}C_{pnf}}\frac{1}{\delta^2}\frac{\partial}{\partial Y_{nf}}\left(\lambda_{nf}\frac{\partial T_{nf}}{\partial Y_{nf}}\right) \tag{5}$$

Conservation of liquid mass flow rate:

$$\int_0^1 \delta \rho_{nf} u_{nf} dY_{nf} = \left[m_{nf} - H\int_0^X \rho v(X, Y = 1)\right]dX \tag{6}$$

2.1.2. For Gas Phase

Continuity equation

$$\frac{\partial \rho u}{\partial X} + \frac{Y-1}{d-\delta}\frac{\partial \delta}{\partial X}\frac{\partial \rho u}{\partial Y} + \frac{H}{d-\delta}\frac{\partial \rho u}{\partial Y} = 0 \tag{7}$$

Momentum equation

$$\begin{aligned} & u\tfrac{\partial u}{\partial X} + \left(u\tfrac{Y-1}{d-\delta}\tfrac{\partial \delta}{\partial X} + v\tfrac{H}{d-\delta}\right)\tfrac{\partial u}{\partial Y} \\ & = -\tfrac{1}{\rho}\tfrac{dp}{dX} - \tfrac{1}{\rho}\tfrac{Y-1}{d-\delta}\tfrac{\partial \delta}{\partial X}\tfrac{\partial p}{\partial Y} - \beta g H(T - T_0) \\ & -\beta^* g H(c - c_0) + \tfrac{1}{\rho}\tfrac{H}{(d-\delta)^2}\tfrac{\partial}{\partial Y}\left(\mu\tfrac{\partial u}{\partial Y}\right) \end{aligned} \tag{8}$$

Energy equation

$$u\frac{\partial T}{\partial X} + \left(u\frac{Y-1}{d-\delta}\frac{\partial \delta}{\partial X} + v\frac{H}{d-\delta}\right)\frac{\partial T}{\partial Y} = \frac{1}{\rho C_p}\left(\frac{H}{(d-\delta)^2}\right)\frac{\partial}{\partial Y}\left(\lambda\frac{\partial T}{\partial Y}\right) + \rho D\left(c_{pv} - c_{pa}\right)\frac{\partial T}{\partial Y}\frac{\partial c}{\partial Y} \tag{9}$$

Diffusion equation

$$u\frac{\partial c}{\partial X} + \left(u\frac{Y-1}{d-\delta}\frac{\partial \delta}{\partial X} + \frac{H}{d-\delta}v\right)\frac{\partial c}{\partial Y} = \frac{1}{\rho}\frac{1}{(1-\delta)^2}\left(\frac{\partial}{\partial Y}\left(\rho D\frac{\partial c}{\partial Y}\right)\right) \tag{10}$$

Conservation of gas mass flow rate

$$\int_0^1 \rho u(X,Y)(d-\delta)dY = \left[(d-\delta_0)\rho_0 u_0 + H\int_0^X \rho v(X,Y=0)dX\right] \tag{11}$$

2.2. Boundary Conditions

For X = 0 (channel entry)

$$u = u_0;\ T = T_0, c = c_0;\ T_{nf} = T_{nf0};\ \delta(0) = \delta_0;\ \mathrm{u_{nf}} = \mathrm{u_{nf0}} \tag{12}$$

For Y = 1 (dry plate)

$$\left[-\lambda\frac{1}{d-\delta}\frac{\partial T}{\partial Y}\right]_{Y=1} = h(T(X,1)-T_0) \text{ and } \left.\frac{\partial c}{\partial Y}\right)_{Y=1} = 0 \tag{13}$$

For Y = 0 (interface between the two phases) (in the interface y = δ then returning to the Equation (1), y = δ give Y = 0)

For the case where we neglect the normal stress forces

$$\frac{1}{d-\delta}\mu\left(\frac{\partial u}{\partial Y}\right)_{Y=0} = \frac{1}{\delta}\mu_{nf}\left(\frac{\partial u}{\partial Y_{nf}}\right)_{Y_{nf}=1} \tag{14}$$

The equality of the velocity for the two phases

$$u(X,Y=0) = u_{nf}\left(X, Y_{nf}=1\right) \tag{15}$$

We consider that the film thickness variation is negligible, and the rate of phase change is small: (interface between the two phases) (in the interface y = 0 then returning to the Equation (1), y = δ give Y = −1)

$$v(X,Y=0) = \left(\frac{D}{1-c(X,0)}\frac{1}{(d-\delta)}\frac{\partial c}{\partial Y}\right)_{(Y=0)} \tag{16}$$

$$T(X,Y=0) = T_{nf}\left(X, Y_{nf}=1\right),\ c(X,Y=0) = c_{sat}(T(X,Y=0) \tag{17}$$

$$-\frac{1}{\delta}\lambda_{nf}\left(\frac{\partial T_{sw}}{\partial Y_{nf}}\right)_{Y_{nf}=1} = -\lambda\frac{1}{d-\delta}\left(\frac{\partial T}{\partial Y}\right)_{Y=0} - \frac{1}{d-\delta}\frac{\rho L_v\left(D+\overline{D}\right)}{(1-c(X,1))}\left(\frac{\partial c}{\partial Y}\right)_{Y=0} \tag{18}$$

For Y_{nf} = −1 (heated plate), regarding the Equation (2)

$$u_{nf} = 0, -\lambda_{nf}\left(\frac{\partial T_{nf}}{\partial Y}\right)_{Ynf=0} = q_w \tag{19}$$

where $c_{sat}(T(x,Y=0)) = \frac{M_v P_{vs}}{M_v P_{vs} - M_a(p-p_{vs})}$ is a vapor concentration at saturation. P_{vs} is a vapor pressure at saturation (Vachon [16]).

In addition, we define the local evaporation rate m(X) and the total evaporation rate at the interface m_t at the axial location X as:

$$m(X) = \frac{\rho D}{1-c(X,0)}\frac{1}{d-\delta}\left(\frac{\partial c}{\partial Y}\right)_{Y=0} \tag{20}$$

$$m_t(X) = \int_0^X m(X)dX \tag{21}$$

The global mass balance at each section and the boundary conditions closes the mathematical system. The present problem defined by the system of equations with the boundary conditions is

solved numerically using a finite difference marching procedure in the downstream direction. A fully implicit scheme where the axial convection terms are approximated by the upstream difference, and the transverse convection and diffusion terms by the central difference is employed. The simulations are to describe the effect of alumina volume rate on the transfers. Particular attention is given to show the efficiency of the alumina content on the phase change temperature.

2.3. Thermophysical properties

All the thermophysical properties of the nano film are obtained from [14,18].

For the thermal conductivity and the dynamic viscosity, we use the empirical correlations of Mintsa et al. [18]:

- $\lambda_{nf} = \lambda_{water}(1.72x_v + 1)$
- $\mu_{nf} = \mu_{water}(123x_v^2 + 7.3x_v + 1)$

For the density, specific heat, and the volume expansion coefficient, we use the usual rules of mixture [14]:

- $\rho_{nf} = (1 - x_v)\,\rho_{water} + x_v\rho_n$
- $(\rho C_p)_{nf} = (1 - x_v)(\rho C_p)_{water} + x_v(\rho C_p)_n$
- $(\rho\beta)_{nf} = (1 - x_v)(\rho\beta)_{water} + x_v(\rho\beta)_n$
- $(\rho\beta^*)_{nf} = (1 - x_v)(\rho\beta^*)_{water} + x_v(\rho\beta^*)_n$

The thermophysical properties of water and the gas mixture are obtained from [19]

2.4. Validation and Mesh Stability

The validations are down under the following conditions: (q_w = 1000 w/m^2, T_0 = 20 °C, T_{nf} = 20 °C, d = 0.015 m, H = 0.2 m, u_0 = 0.5 m/s, relative humidity equal to 50% and m_{0L} = 0.01 kg·m^{-1}s^{-1}). A comparison is made with Yan et al. [17]. Figure 2 shows that the relative difference between our results and those obtained by Yan [17] is lower than 8% for the interfacial temperature. These discrepancies cold be explained by the difference between the physical properties used in the two works and the effect of convection terms neglected by Yan [17] in the liquid phase. For the mesh stability as mention in Table 1, a maximum variation observed is less than 1% for the interfacial temperature. To reduce the cost of computation, we choose the grid 71 × 5l × 21 in this study.

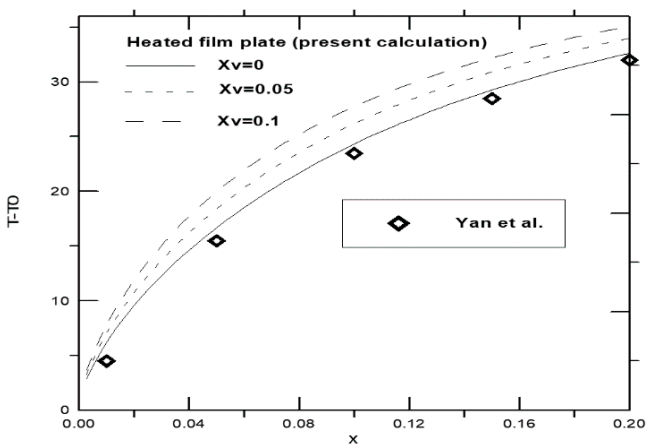

Figure 2. Validation of the code simulation. Interfacial temperature – comparison with Yan et al. [17].

Table 1. Stability of calculation from a mesh variations-interfacial temperature.

POSITION AXIALE	(121,121,81)	(121,121,21)	(121,51,41)	(121,51,21)	(71,51,21)	(51,41,21)
X = 0.2	333.73	333.65	333.45	333.42	333.60	333.39
X = 0.4	334.96	334.92	334.81	334.73	334.91	334.69
X = 0.6	337.43	337.39	337.29	337.22	337.12	337.36
X = 0.8	339.06	339.02	338.88	338.77	338.71	338.98
X = 1.0	340.35	340.31	340.18	340.11	340.02	340.28

3. Results and Discussions

We study the evaporation of liquid film by the mixed convection of a humid air. This liquid film is falling down on one of two vertical channel plates, which is heated. The second plate is dry and exchanges heat with the outlet with a certain heat transfer coefficient h = 15w/Km^2. In this study, we present the effect of the nano fluid volume rate on the transfers when the film plate is heated. The simulations are done under the following conditions: (T_0 = 25 °C, T_{nf} = 25 °C, d = 0.015 m, H = 3 m, u_o = 1 m/s, c_0 = 0 and m_{0L} = 0.01 kg·m^{-1}s^{-1}).

At present, the film plate is heated by a uniform heat flux q_w = 1000 W/m^2. Figure 3 shows the effect of the volume rate of the nanoparticle on the channel temperature at the exit. Because of the heating, the effect of the thermal conduction is significant and dominate the effect of density and the specific heat. At seen in Equations (9) and (17), an augmentation of the thermal conductivity induces an increase of the film temperature. Also, it augments interfacial temperature (Figure 4) and consequently the vapor temperature. This augmentation of k exists because of the increasing of x_v [14]. The saturation vapor concentration increases when we elevate the nanoparticle volume rate (Vachon [16]). This is shown in Figure 5. Figure illustrates the effect of an increasing of the nanoparticle volume rate on the evaporation production. As a consequence of interfacial vapor concentration, the gradient of concentration near the interface is elevated. This increases naturally the evaporation rate (Figure 6). The augmentation of the film density, due to the x_v increasing [14], induces a deceleration of the film (Equation (8)) as shown in Figure 7. The thermal conductivity doesn't affect the convection of the film (see the equation of momentum of the nano film—Equation (8)).

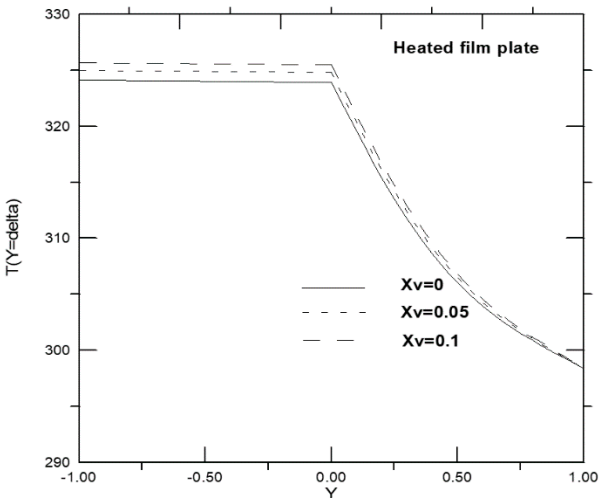

Figure 3. Effect of the nanoparticle volume rate on the exit channel temperature – heated plate case.

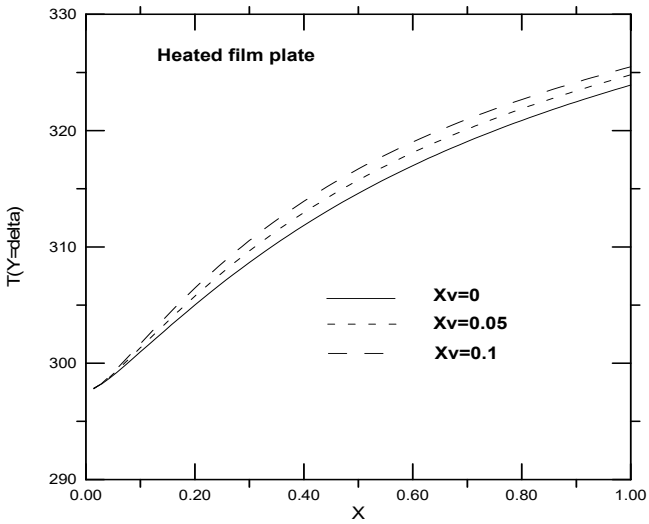

Figure 4. Effect of the nanoparticle volume rate on the interfacial temperature – heated plate case.

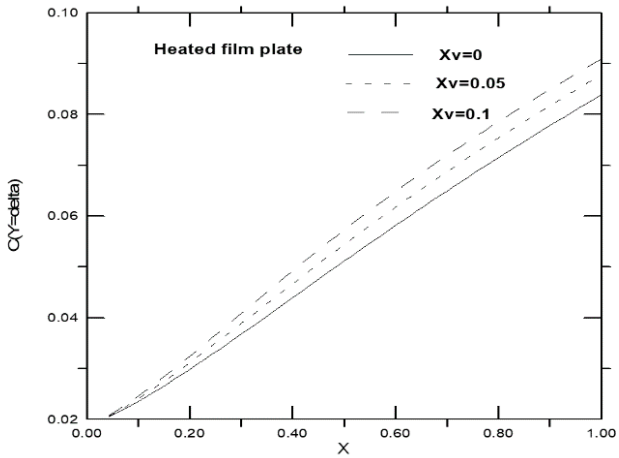

Figure 5. Effect of the nanoparticle volume rate on the interfacial vapor concentration – heated plate case.

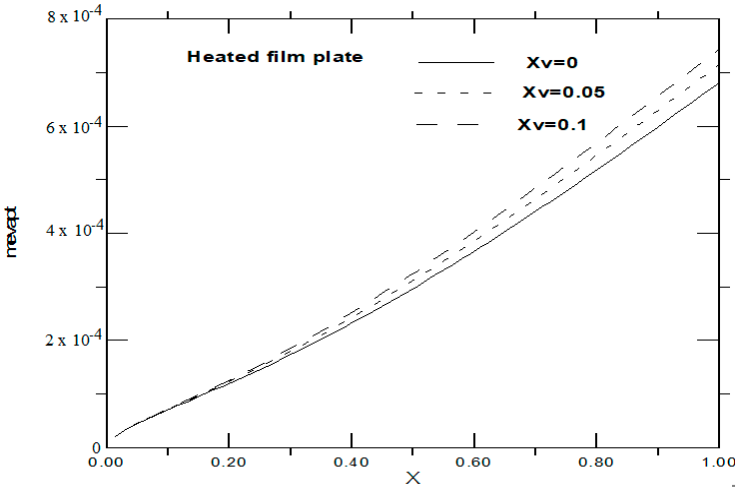

Figure 6. Effect of the nanoparticle volume rate on the total evaporation rate-heated plate case.

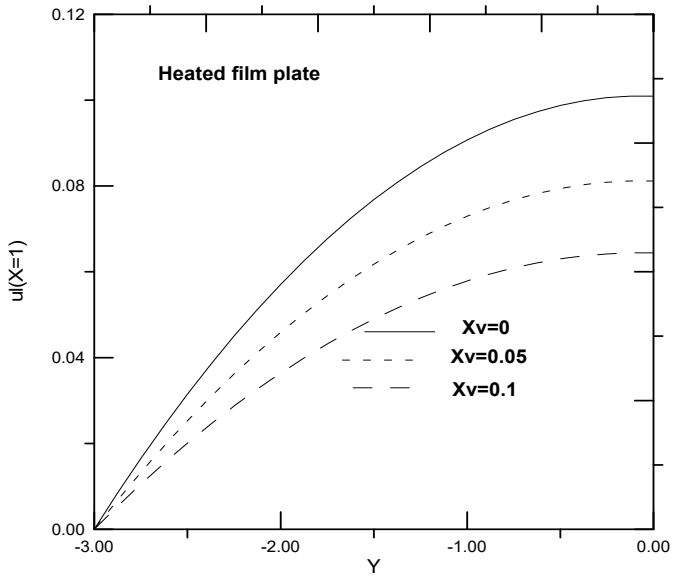

Figure 7. Effect of the nanoparticle volume rate on the film velocity – heated plate case.

4. Conclusions

We performed a study of a Nano film of alumina–water flowing on a heated plate of a vertical channel. Validation and stability study of the mesh is given after mathematical analysis. Also, we have paid attention to prove the important influence of heating on the volume rate of the nanoparticle. Simulations provide the following conclusions:

- The effect of the thermal conduction is significant and dominates the effect of density and the specific heat.
- An augmentation of the thermal conductivity induces an increase of the film temperature and the interfacial temperature, and consequently the vapor temperature.
- Augmentation of k exists because of the increase of x_v.
- The saturation vapor concentration is elevated when we elevate the nanoparticle volume rate.
- Augmentation of k naturally increases the evaporation rate.
- The augmentation of the film density, due to the increase of x_v, induces a deceleration of the film.

Author Contributions: A.B.M., W.H. and I.T. developed the design strategy and design the interview questions. A.B.M., W.H. and I.T. collected the data and A.B.M., W.H. and I.T. analyzed the data. The results were finalized by A.B.M., W.H. and I.T. and A.B.M., W.H. and I.T. formulated the paper draft and wrote the manuscript A.B.M., W.H. and I.T. helped to review and finalize the manuscript. All authors have read and agreed to the published version of the manuscript.

Funding: This research received no external funding.

Conflicts of Interest: The authors declare no conflicts of interest.

List of Symbols

u	axial velocity [m/s]
v	v transversal velocity [m/s]
p	p pressure [Pa]
x	axial coordinate [m]
y	transversal coordinate [m]
X	axial dimensionless coordinate
Y	transversal dimensionless coordinate
T	temperature [°K]
g	gravitational acceleration [m/s^2]
h	heat transfer coefficient at the dry plate [J/m^2·K]

c	mass fraction vapor
D	diffusivity [m^2/s]
m_{nf0}	inlet mass flow rate [kg/m.s]
$m_t(X)$	total evaporation rate [kg/s]
N_{ynf}	knot number in y direction for liquid
N_y	knot number in y direction for gas
L_v	latent heat per mass unit
d	channel width [m]
H	channel length [m]
x_v	Nano particle volume rate [ppm]
Greek symbols	
ρ	density [kg/m^3]
μ	dynamic viscosity [kg/ms]
λ	thermal conductivity [W/mK]
δ	film thickness [m]
β	thermal expansion coefficient $-1/\rho(\partial\rho/\partial T)_{p,c}$ [K^{-1}]
β*	mass expansion coefficient $-1/\rho(\partial\rho/\partial c)_{p,T}$

Subscripts

0	inlet condition
i	interface
n_f	nano fluid

References

1. Plawsky, J.L.; Ojha, M.; Chatterjee, A.; Wayner, P.C., Jr. Review of the effects of surface topography, surface chemistry, and fluid physics on evaporation at the contact line. *Chem. Eng. Commun.* **2009**, *196*, 658–696. [CrossRef]
2. Wang, B.X.; Garimella, S.V.; Murthy, J.Y. An analytical solution for the total heat transfer in the thin-film region of an evaporating meniscus. *Int. J. Heat Mass Transf.* **2008**, *51*, 6317–6322. [CrossRef]
3. Do, K.H.; Jang, S.P. Effect of nanofluids on the thermal performance of a flat micro heat pipe with a rectangular grooved wick. *Int. J. Heat Mass Transf.* **2010**, *53*, 2183–2192. [CrossRef]
4. Zhao, J.-J.; Duan, Y.-Y.; Wang, X.-D.; Wang, B.-X. Effect of nanofluids on thin film evaporation in microchannels. *J. Nanopart. Res.* **2011**, *13*, 5033–5047. [CrossRef]
5. Choi, S. Enhancing thermal conductivity of fluids with nanoparticles. *Asme Fed.* **1995**, *231*, 100–103.
6. Lee, S.; Choi, S.S.; Li, S.; Eastman, J.A. Measuring thermal conductivity of fluids containing oxide nanoparticles. *J. Heat Transf.* **1999**, *121*, 280–289. [CrossRef]
7. Xuan, Y.; Li, Q. Heat transfer enhancement of nanofluids. *Int. J. Heat Fluid Flow* **2000**, *21*, 58–64. [CrossRef]
8. Xuan, Y.; Roetzel, W. Conceptions for heat transfer correlation of nanofluids. *Int. J. Heat Mass Transf.* **2000**, *43*, 3701–3707. [CrossRef]
9. Ali, A.; Vafai, K.; Khaled, A.R. Analysis of heat and mass transfer between air and falling film in a cross flow configuration. *Int. J. Heat Mass Transf.* **2004**, *47*, 743–755. [CrossRef]
10. Pak, B.C.; Cho, Y.I. Hydrodynamic and heat transfer study of dispersed fluids with submicron metallic oxide particles. *Exp. Heat Transf.* **1998**, *11*, 151–170. [CrossRef]
11. Li, Q.; Xuan, Y. Convective heat transfer performances of fluids with nanoparticles. In Proceedings of the 12th International Heat Transfer Conference, Grenoble, France, 18–23 August 2002; pp. 483–488.
12. Wen, D.; Ding, Y. Experimental investigation into convective heat transfer of nanofluids at the entrance region under laminar flow conditions. *Int. J. Heat Mass Transf.* **2004**, *47*, 5181–5188. [CrossRef]
13. Yang, Y.; Zhang, Z.G.; Grulke, E.A.; Anderson, W.B.; Wu, G. Heat transfer properties of nanoparticle-in-fluid dispersions (nanofluids) in laminar flow. *Int. J. Heat Mass Transf.* **2005**, *48*, 1107–1116. [CrossRef]
14. Fohanno, S.; Polidori, G.; Popa, C. *Nanofluides et transfert de chaleur par convection naturelle*; Journée Thématique SFT: Paris, France, 15 March 2012.

15. Cherif, A.A.; Daif, A. Etude numérique du transfert de chaleur et de masse entre deux plaques planes verticales en présence d'un film de liquide binaire ruisselant sur l'une des plaques chauffée. *Int. J. Heat Mass Transf.* **1999**, *42*, 2399–2418. [CrossRef]
16. Vachon, M. Etude De L'évaporation En Convection Naturelle. Ph.D. Thesis, Université De Poitiers, Grand Poitiers, France, 1979.
17. Yan, W.M. Effects of film evaporation on laminar mixed heat ad mass tansfer in a vertical channel. *Int. J. Heat Mass Transfer* **1992**, *35*, 3419–3429.
18. Mintsa, H.A.; Roy, G.; Nguyen, C.T.; Doucet, D. New temperature dependent thermal conductivity data for water-based nanofluids. *Int. J. Therm. Sci.* **2009**, *48*, 363–371. [CrossRef]
19. Agunaoun, A.; Daif, A.; Baniol, R.; Dagunet, M. Evaporation en convection forcée d'un film mince s'écoulant en régime permanent, laminaire et sans ondes, sur une surface plane inclinée. *Int. J. Heat Md Mass Transf.* **1994**, *37*, 2947–2956. [CrossRef]
20. Chen, R.H.; Phuoc, T.X.; Martello, D. Surface tension of evaporating nanofluid droplets. *Int. J. Heat Mass Transf.* **2011**, *54*, 2459–2466. [CrossRef]
21. Orejon, D.; Sefiane, K.; Shanahan, M.E.R. Evaporation of nanofluid droplets with applied DC potential. *J. Colloid Interface Sci.* **2013**, *407*, 29–38. [CrossRef]
22. Ni, G.; Miljkovic, N.; Ghasemi, H.; Huang, X.; Boriskina, S.V.; Lin, C.; Wang, J.; Xu, Y.; Rahman, M.M.; Zhang, T.J.; et al. Volumetric solar heating of nanofluids for direct vapor generation. *Nano Energy* **2015**, *17*, 290–301. [CrossRef]
23. Amjad, M.; Raza, G.; Xin, Y.; Pervaiz, S.; Xu, J.; Du, X.; Wen, D. Volumetric solar heating and steam generation via gold nanofluids. *Appl. Energy* **2017**, *206*, 393–400. [CrossRef]
24. Zhou, Y.; Li, Q.; Wang, Q. Energy Storage Analysis of UIO-66 and Water Mixed Nanofluids: An Experimental and Theoretical Study. *Energies* **2019**, *12*, 2521. [CrossRef]
25. Moshizi, S.A. Forced convection heat and mass transfer of MHD nanofluid flow inside a porous microchannel with chemical reaction on the walls. *Eng. Comput.* **2015**, *32*, 2419–2442. [CrossRef]
26. Moshizi, S.A.; Malvandi, A.; Ganji, D.D.; Pop, I. A two-phase theoretical study of Al_2O_3-water nanofluid flow inside a concentric pipe with heat generation/absorption. *Int. J. Therm. Sci.* **2014**, *84*, 347–357. [CrossRef]
27. Moshizi, S.A. Conjugated effect of joule heating and magnetohydrodynamic on laminar convective heat transfer of nanofluid inside annulus pipe in the presence of slip condition. *Int. J. Thermophys.* **2016**, *37*, 1–22. [CrossRef]
28. Moshizi, S.A.; Malvandi, A. Magnetic field Effects on nanoparticle migration at mixed convection of nanofluids in microchannels with temperature-dependent thermophysical properties. *J. Taiwan Inst. Chem. Eng.* **2016**, *66*, 269–282. [CrossRef]
29. Moshizi, S.A.; Malvandi, A. Different modes of nanoparticle migration at mixed convection of Al_2O_3–water nanofluid inside a vertical microannulus in the presence of heat generation/absorption. *J. Therm. Anal. Calorim.* **2016**, *126*, 1947–1962. [CrossRef]
30. Moshizi, S.A.; Zamani, M.; Hosseini, S.J.; Malvandi, A. Mixed convection of magnetohydrodynamic nanofluids inside microtubes at constant wall temperature. *J. Magn. Magn. Mater.* **2017**, *430*, 36–46. [CrossRef]
31. Malvandi, A.; Moshizi, S.A.; Ganji, D.D. Nanoparticle transport effect on magnetohydrodynamic mixed convection of electrically conductive nanofluids in micro-annuli with temperature-dependent thermophysical properties. *Phys. E Low Dimens. Syst. Nanostruct.* **2017**, *88*, 35–49. [CrossRef]
32. Sohail1, M.; Naz, R.; Abdelsalam, S. On the onset of entropy generation for a nanofluid with thermal radiation and gyrotactic microorganisms through 3D flows. *Phys. Scr.* **2020**, *95*, 4. [CrossRef]
33. Eldesoky, I.M.; Abdelsalam, S.I.; El-Askary, W.A.; Ahmed, M.M. Concurrent development of thermal energy with magnetic field on a particle-fluid suspension through a porous conduit. *BioNanoScience* **2019**, *9*, 186–202. [CrossRef]
34. Abdelsalam, S.I.; Bhatti, M.M. The study of non-Newtonian nanofluid with hall and ion slip effects on peristaltically induced motion in a non-uniform channel. *Rsc Adv.* **2018**, *8*, 7904–7915. [CrossRef]